Biotechnology Reports 14 (2017) 38–46

Contents lists available at ScienceDirect

Biotechnology Reports

journal homepage: www.elsevier.com/locate/btre

High sucrolytic activity by invertase immobilized onto magnetic diatomaceous earth nanoparticles

Mariana P. Cabrera[a,b], Caio R.D. Assis[a], David F.M. Neri[c], Claudete F. Pereira[d], Fernando Soria[b], Luiz B. Carvalho Jr.[a,*]

[a] Departamento de Bioquímica e Laboratório de Imunopatologia Keizo Asami (LIKA), Universidade Federal de Pernambuco, Cidade Universitária, 50670-901, Recife, PE, Brazil
[b] Instituto de Investigaciones para la Industria Química (INIQUI), Universidad Nacional de Salta – CONICET, 4400, Salta, Argentina
[c] Instituto de Pesquisa em Ciência dos Materiais, Universidade Federal do Vale do São Francisco, 48920-310, Juazeiro, BA, Brazil
[d] Departamento de Química Fundamental, Universidade Federal de Pernambuco, Cidade Universitária, 50740-560, Recife, PE, Brazil

ARTICLE INFO

Keywords:
Immobilization
Invertase
Sucrolytic activity
Magnetic particle
Diatomaceous earth

ABSTRACT

Invertase immobilized on magnetic diatomaceous earth nanoparticles (mDE-APTES-invertase) with high sucrolytic activity was obtained by an easy and low-cost method. An experimental design was carried out to investigate the best immobilization conditions and it allowed obtaining an immobilized derivative with a residual specific activity equal to 92.5%. Then, a second experimental design selected the mDE-APTES-invertase with higher specific activity in relation to other derivatives reported in the literature (2.42-fold). Thermal and storage stability for immobilized invertase were found to be 35 °C for 60 min (85% retained activity) and 120 days storage period (80% retained activity), respectively. Besides, a residual activity higher than 60% and 50% were observed for mDE-APTES-invertase after reuse in short and long term, respectively. Given the simple and efficient method to obtain an immobilized derivative with high activity, the mDE nanoparticles appear to be a promising matrix for invertase immobilization as well as for other biomolecules.

1. Introduction

Immobilized enzymes have been widely used in the biotechnology. These biocatalysts have presented some advantages such as thermal stability, easy separation from reactor and reuse. These benefits lead to a reduction of process costs [1]. The industrial use of immobilized enzymes requires the evaluation of variables that may affect their activities in order to optimize their performance [2]. Invert sugar is a valuable commercial product for the food industry in countries where the main sources of sugar are beet or cane. The free and immobilized invertase (EC 3.2.1.26) produces high quality invert sugar with low concentrations of 5-hydroxymethyl-2-furfural (HMF – a carcinogenic byproduct) and without color development compared to the colored version obtained through acid hydrolysis [3,4]. Invertase is one of the most studied enzymes and it has been immobilized by different methods and supports [5–8].

Magnetic bio-separation technology is an attractive strategy for recovering magnetic immobilized enzymatic derivatives. These composites under nanoparticles sizes add the advantage of high surface to volume ratio such as the immobilized invertase on chitosan coated γ-Fe_2O_3 magnetic nanoparticles [7]. Diatomaceous earth (DE) or diatomite is a naturally occurring clay from geological deposits composed predominantly of the fossilized skeletons of diatoms. These organisms constitute an abundant and inexpensive source of silica [9]. DE typically consists of 87–94% silicon dioxide (SiO_2) with significant quantities of alumina (Al_2O_3) and ferric oxide (Fe_2O_3) [10,11]. They present interesting properties such as porous structure, high silica content, low density, high surface area, low conductivity coefficient and are chemically inert. DE has numerous applications as filter media, adsorbent, catalyst support or carrier, natural insecticide or grain protectant [10,12]. Magnetic diatomaceous earth (mDE) has been explored in magnetic bio-separation technology [13–17]. However, these applications do not include enzyme immobilization that was firstly employed for invertase in our lab [18].

In this study, mDE nanoparticles were proposed as a matrix for protein immobilization using invertase as enzyme model. In addition, our main goal was to investigate the immobilization process as well as the best conditions of the sucrose hydrolysis by the immobilized derivative through the design of experiments. Physicochemical characterization of the matrix and the immobilized invertase functionality,

* Corresponding author at: Laboratório de Imunopatologia Keizo Asami (LIKA), Universidade Federal de, Pernambuco, Cidade Universitária, Recife – PE, CEP 50670-901, Brazil.
E-mail address: lbcj.br@gmail.com (L.B. Carvalho).

http://dx.doi.org/10.1016/j.btre.2017.03.001
Received 11 January 2017; Received in revised form 25 March 2017; Accepted 29 March 2017
Available online 06 April 2017

such as thermal stability, storage stability, shelf life and reuse, were also performed. All the results obtained in this work would provide a sound basis for further exploration.

2. Materials and methods

2.1. Materials

Diatomaceous earth (DE) was kindly supplied by TAMER S.A. (Salta, Argentina). A process of water washing and repeated sedimentation was applied to purify the raw DE. Invertase from Baker's yeast (178.8 U mg^{-1} protein), aminopropyltriethoxysilane (APTES), glutaraldehyde and bovine serum albumin (BSA) were purchased from Sigma Aldrich Chemicals (St. Louis, USA). All other chemicals were of high purity available commercially.

2.2. Diatomaceous earth magnetization

Magnetic DE nanoparticles (grain size around of 12 nm) were synthesized as reported by Cabrera et al. [18]. Briefly, 5 mL of iron solutions (0.6 mol L^{-1} $FeCl_2{\cdot}4H_2O$ and 1.1 mol L^{-1} $FeCl_3{\cdot}6H_2O$) were added to DE preparation (2.0% w/v). The final pH magnetization was adjusted with ammonium hydroxide (7.6 mol L^{-1}) up to 11.0. After this, magnetic solution was kept under stirring for 30 min at 100 °C. The magnetic diatomaceous earth (mDE) obtained (black precipitate) was washed with distilled water until pH 7.0 by using a magnetic field (Ciba Corning; 0.6 T). The mDE nanoparticles were stored at 25 °C until later use. This magnetic preparation is economically attractive due to the low cost of the diatomaceous earth found in natural resource as well as the co-precipitation method for magnetite nanoparticles synthesis is also very simple and fast.

2.3. Invertase immobilization on mDE-APTES: 1st Experimental design

The mDE functionalization with APTES/glutaraldehyde, and posterior immobilization process were investigated using design of experiments (DOE). This statistical analysis is a structured and systematized method of experimentation in which all factors are varied simultaneously over a set of experimental runs [19]. Here, we used this method to identify the effects of several variables on the mDE functionalization and invertase immobilization process. Thus, a 2_{IV}^{7-2} fractional factorial design including seven variables with two levels namely low (−1) and high (+1) was employed. The variables under study were: APTES concentration, APTES contact time, glutaraldehyde concentration, glutaraldehyde contact time, immobilization time, immobilization pH and invertase concentration. Table 1 shows the range of the studied variables and the experimental runs. The sequence of experiments was randomized in order to minimize the effects of the uncontrolled factors.

Preparation of mDE-APTES. The mDE nanoparticles (0.10 g) were submerged in a silane coupling agent solution (2 mL APTES, prepared in acetone) and stirred at 25 °C. Next, the mDE nanoparticles treated with APTES (mDE-APTES) were washed with distilled water and recovered using magnetic field (0.6 T).

Preparation of mDE-APTES-invertase. Firstly, the activation of the mDE-APTES (0.01 g) with glutaraldehyde (2 mL) prepared in 0.2 mol L^{-1} sodium acetate buffer pH 5.0, from now on called buffer, at 25 °C was also necessary to immobilize the enzyme by covalent binding. The mDE-APTES activated with glutaraldehyde was washed several times with distilled water and buffer until the washings became colorless. After this, invertase solution (1 mL, prepared in buffer) was incubated with mDE-APTES activated (0.01 g) at 4 °C under mild stirring for different times (see Table 1). The washing procedure was repeated for five times with buffer. The invertase immobilized on mDE-APTES (mDE-APTES-invertase) was collected using external magnetic field and the supernatants including the first two washings were used for protein determination according to Lowry et al. [20] using BSA as standard. The amount of immobilized protein was calculated by the difference between the offered protein and that found in the supernatants and washings. The mDE-APTES-invertase was stored in buffer at 4 °C for further use. The immobilization pH and time were also investigated in order to study their influences in the immobilization process (see Table 1). For this, invertase solutions were prepared at different pH (0.2 mol L^{-1} sodium acetate buffer), and immobilization time was set up according to the time variation in the procedure of immobilization.

Table 1
Experimental design for the mDE functionalization processes and the covalent immobilization of enzyme.

Variables	Factor code	Unit	Variables levels	
			−1	+1
[APTES]	X_1	%	2.5	10.0
APTES contact time	X_2	h	1	2
[Glutaraldehyde]	X_3	%	2.5	10.0
Glutaraldehyde contact time	X_4	h	1	2
Immobilization time	X_5	h	2	12
Immobilization pH	X_6	–	4.0	5.5
[Invertase]	X_7	mg mL^{-1}	0.05	0.15

Run	X_1	X_2	X_3	X_4	X_5	X_6	X_7	Y^a	Y^b
1	−1	−1	−1	−1	-1	+1	+1	36	0.330
2	+1	−1	−1	−1	-1	-1	-1	100	0.057
3	−1	+1	−1	−1	-1	-1	-1	100	0.093
4	+1	+1	−1	−1	-1	+1	+1	47	0.616
5	−1	−1	+1	−1	-1	-1	+1	88	0.182
6	+1	−1	+1	−1	-1	+1	-1	80	0.199
7	−1	+1	+1	−1	-1	+1	-1	83	0.278
8	+1	+1	+1	−1	-1	-1	+1	87	0.085
9	−1	−1	−1	+1	-1	-1	-1	100	0.094
10	+1	−1	−1	+1	-1	+1	+1	27	0.354
11	−1	+1	−1	+1	-1	+1	+1	34	0.324
12	+1	+1	−1	+1	-1	-1	-1	100	0.057
13	−1	−1	+1	+1	-1	+1	-1	92	0.532
14	+1	−1	+1	+1	-1	-1	+1	94	0.185
15	−1	+1	+1	+1	-1	-1	+1	98	0.183
16	+1	+1	+1	+1	-1	+1	-1	91	0.102
17	−1	−1	−1	−1	+1	+1	-1	100	0.100
18	+1	−1	−1	−1	+1	-1	+1	79	0.209
19	−1	+1	−1	−1	+1	-1	+1	79	1.043
20	+1	+1	−1	−1	+1	+1	-1	66	0.420
21	−1	−1	+1	−1	+1	-1	-1	100	0.735
22	+1	−1	+1	−1	+1	+1	+1	27	0.626
23	−1	+1	+1	−1	+1	+1	+1	36	0.886
24	+1	+1	+1	−1	+1	-1	-1	100	0.481
25	−1	−1	−1	+1	+1	-1	+1	75	0.251
26	+1	−1	−1	+1	+1	+1	-1	72	0.701
27	−1	+1	−1	+1	+1	+1	-1	73	0.765
28	+1	+1	−1	+1	+1	-1	+1	78	0.330
29	−1	−1	+1	+1	+1	+1	+1	27	0.620
30	+1	−1	+1	+1	+1	-1	-1	100	0.694
31	−1	+1	+1	+1	+1	-1	-1	100	0.566
32	+1	+1	+1	+1	+1	+1	+1	28	0.493

Y^a corresponds to the immobilized protein percentage.
Y^b corresponds to the response: enzymatic activity (U mg^{-1} support).

2.4. Sucrose hydrolysis by mDE-APTES-invertase: 2nd Experimental design

To perform the present statistical study, the experimental conditions used in the functionalization and immobilization processes were corresponding to the best run of the first experimental design. A 2^4 complete factorial design with central point was performed to investigate the best conditions of sucrose hydrolysis by mDE-APTES-invertase. This approach enabled an experimental investigation of the individual factors and the interactions of the factors simultaneously as opposed to one factor at-a-time approach. The independent variables studied were:

Table 2
Experimental design for the sucrose hydrolysis by mDE-APTES-invertase.

Variables	Factor code	Unit	Variables levels		
			−1	0	+1
pH	X_1	–	4.5	5.0	5.5
Temperature	X_2	°C	45	55	65
[Sucrose]	X_3	mol L^{-1}	0.15	0.20	0.25
[Invertase]	X_4	mg mL^{-1}	0.05	0.10	0.15

Run	X_1	X_2	X_3	X_4	Y^a
1	−1	−1	−1	−1	59.21
2	+1	−1	−1	−1	36.93
3	−1	+1	−1	−1	36.87
4	+1	+1	−1	−1	27.90
5	−1	−1	+1	−1	100.00
6	+1	−1	+1	−1	48.11
7	−1	+1	+1	−1	31.38
8	+1	+1	+1	−1	43.23
9	−1	−1	−1	+1	13.02
10	+1	−1	−1	+1	12.86
11	−1	+1	−1	+1	1.90
12	+1	+1	−1	+1	9.07
13	−1	−1	+1	+1	13.63
14	+1	−1	+1	+1	16.96
15	−1	+1	+1	+1	6.46
16	+1	+1	+1	+1	16.98
17	0	0	0	0	23.57
18	0	0	0	0	30.15
19	0	0	0	0	30.10

Y^a corresponds to the response: percentage specific activity. It was estimated from the most value of specific activity (3358 U mg^{-1} protein) of the mDE-APTES-invertase and was considered as 100%.

pH, temperature, sucrose concentration and invertase concentration, and the percentage specific activity was used as dependent variable. Table 2 shows the independent variables (factors) and their levels, and the dependent variable (response). The experiments were carried out randomized.

2.5. Statistical data analysis

All the statistical analysis was carried out using *Statistica 12® StatSoft*. The level of significance was set at $p < 0.05$.

2.6. Enzyme assay

Invertase activity was determined by using 0.15 mol L^{-1} sucrose (10 mL) prepared in buffer. After 15 min of incubation at 25 °C, 20 μL of the sample was withdrawn and added to 2.0 mL of working solution in order to measure released glucose using a glucose oxidase-peroxidase (GOD/POD) enzymatic kit (Doles, Goiás, Brazil). One unit of enzyme activity (U) was defined as the amount of enzyme releasing 1 μmol of glucose per minute per mL under the assay conditions.

2.7. Thermal stability

The thermal stability of the free and immobilized invertase were carried out by measuring the residual activity (%) of the enzyme pre-incubated at different temperatures (35–55 °C) in buffer for 30–120 min. After cooling (25 °C), the enzyme activity was determined as previously described in the Section 2.6.

2.8. Storage stability

Storage stability of mDE-APTES-invertase was studied for a period of 120 days at 4 °C. The specific activity of the immobilized derivative was established from time to time using different samples, with sucrose (0.25 mol L^{-1}) as substrate by the method described in Section 2.6.

2.9. Reusability of the mDE-APTES-invertase: short and long term

To assess the performance in short and long term, the mDE-APTES-invertase was reused ten times at 30 min interval, and six times during 120 days, respectively. The residual activity (%) was measured with sucrose (0.25 mol L^{-1}) as substrate. After assay, immobilized preparation was washed with buffer, magnetically collected for the next activity cycle and stored at 4 °C.

2.10. Characterization

The morphological characterization of samples was carried out with a scanning electron microscope (SEM, FEI Model QUANTA 200 FEG) equipped with energy dispersive spectroscopy (EDS). The samples were coated with gold prior to analysis. The identification of the chemical elements present in the material was performed by EDS. Fourier transformed infrared (FTIR) spectra in the 4000–400 cm^{-1} range were recorded for all samples in a BRUKER instrument model IFS 66. The samples were pressed into pellets with KBr. The specific surface area and the porosity were determined for all materials with a Micromeritics ASAP 2420 porosimeter. The isotherms were obtained at 77 K using N_2 as an adsorbate. The specific surface area was calculated using the Brunauer-Emmett-Teller (BET) model. Pore size distribution and pore volume were determined from the desorption branch of the isotherms using the Barrett-Joyner-Halenda (BJH)-plot method.

3. Results and discussion

3.1. Study of the immobilization process

A screening of the most important factors, that affect the immobilization process of invertase on mDE-APTES nanoparticles, was carried out through a 2^{7-2}_{IV}fractional factorial design (Table 1). The immobilized protein percentage and the enzymatic activity were the responses used to assess the immobilization process. According to the statistical analysis, based on normal probability plot (at a confidence level of 95%), as shown in Fig. S1 (see Supplementary material) only the immobilization pH, invertase concentration and immobilization time (main factors), and glutaraldehyde concentration*immobilization time (X_3*X_5; interaction factor of second order) were the statistically significant factors. Considering only these four factors, it was possible to perform a new data analysis as a complete factorial (2^4) design with repetition and to estimate the pure error of the measurements conditioned to the results presented in Table 1.

Hereafter, we present the association of the results of both responses in the choice of a unique run with the experimental conditions more suitable for the immobilization process.

As the final result of this fractional factorial design, Fig. 1 shows the scatterplot of both responses: immobilized protein (%) and enzymatic activity (U mg^{-1} support). Analyzing the responses simultaneously were not chosen a main factor or interaction factor as a result of this DOE, but was chosen the best experimental conditions for the immobilization process of invertase using the mDE nanoparticles as a matrix. Thereby, the screening of seven different factors indicated that the runs 19 and 23 presented the best operational conditions for this process. The differences between these runs were the glutaraldehyde concentration and the immobilization pH. The run 19 had the low levels (−) of these parameters whereas the run 23 had the high levels (+) of the same parameters (Table 1). Furthermore, a slight loss of enzymatic activity (1.2-fold) for the run 23 was also observed. The decrease of the immobilized enzyme activity can be ascribed to the multipoint attachment of the enzyme molecules onto the mDE nanoparticles and/or overloading of immobilized enzyme. The degree of activity decrease is mainly dependent on the properties of the support,

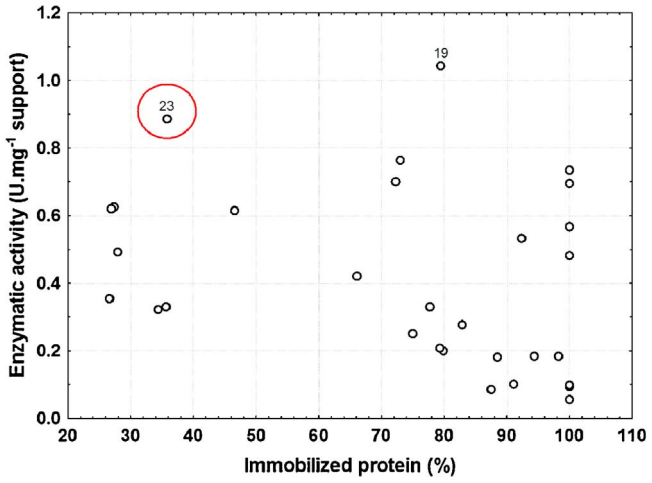

Fig. 1. Scatterplot for both responses: immobilized protein (%) and enzymatic activity (U mg^{-1} support).

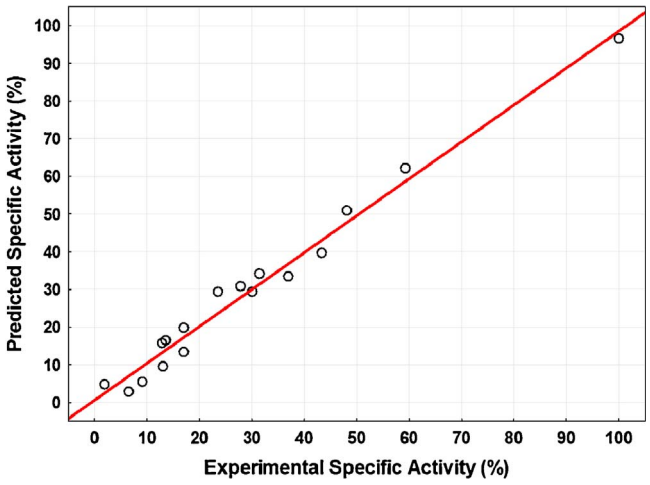

Fig. 3. Predicted specific activity (%) *versus* experimental specific activity (%).

enzyme nature and immobilization conditions/activators.

On the other hand, the immobilized derivatives (mDE-APTES-invertase) of the run 19 and the run 23 presented a residual specific activity equal to 48.9% and 92.5%, respectively. Such values were obtained as percentage of the specific activity of the free enzyme (178.8 U mg^{-1} protein), namely, 87.5 U mg^{-1} protein (run 19) and 165.4 U mg^{-1} protein (run 23), respectively

For this reason, the operational conditions of the run 23 were chosen for the use in the immobilization process: APTES concentration (2.5%), APTES contact time (2 h), glutaraldehyde concentration (10.0%), glutaraldehyde contact time (1 h), immobilization time (12 h), immobilization pH (5.5) and invertase concentration (0.15 mg mL^{-1}). Bergamasco [21] reported a low activity yield around 24% for the immobilized invertase on controlled pore silica particles under the next conditions: APTES concentration (0.5%), APTES contact time (3 h), glutaraldehyde concentration (2.5%), glutaraldehyde contact time (45 min), immobilization time (15 h) and immobilization pH (4.5). Similarly, Sanjay and Sugunan [22] also reported a low retained activity (36%) when the conditions for the invertase immobilization on montmorillonite K10 were: APTES concentration (10%), APTES contact time (1 h), glutaraldehyde concentration (10%), glutaraldehyde contact time (1 h), immobilization time (1 h) and immobilization pH (5.0).

3.2. Sucrose hydrolysis by mDE-APTES-invertase

The effects of sucrose hydrolysis parameters (pH, temperature, sucrose concentration and invertase concentration) on specific activity (%) of the mDE-APTES-invertase were investigated. Fig. 2 shows the Pareto chart of standardized effects that was used to graphically summarize and display the relative importance of the differences between different variables studied in the sucrose hydrolysis process by mDE-APTES-invertase. The length of each bar was proportional to the value of its associated regression coefficient or estimated effect. The chart included a vertical line that corresponded to the 95% limit indicating statistical significance. A factor was, therefore, significant if its corresponding bar crossed this vertical line [23]. According to the Pareto chart of standardized effects (Fig. 2), three main factors (X_2, X_3 and X_4) and interactions factors of second order (X_1X_2, X_1X_4 and X_2X_4) were statistically significant ($p < 0.05$). It is evident that temperature (X_2) and invertase concentration (X_4) were the most significant variables in the sucrose hydrolysis process. The negative effects of these factors indicated that low level for the temperature and invertase concentration favored the response variable (percentage specific activ-

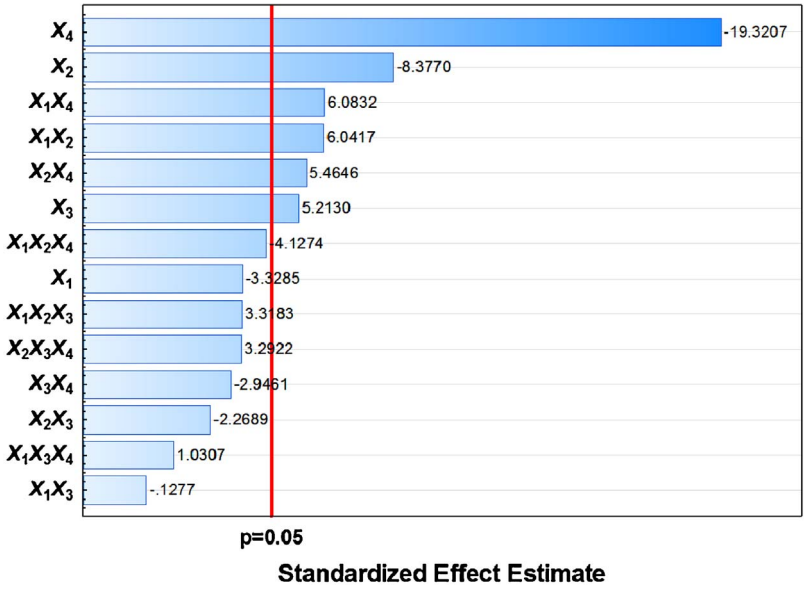

Fig. 2. Pareto chart of standardized effects for the full design experiment, where X_1, X_2, X_3 and X_4 are pH, temperature, sucrose concentration, and invertase concentration, respectively. The line indicates the confidence level of 95%, and factors with standardized effect values to the right of this line are statistically significant.

Table 3
Comparison of the sucrose hydrolysis conditions for immobilized invertase on different supports and immobilization methods.

Support	Immobilization method	Specific activity (U mg^{-1}protein)[a]	pH	Temperature (°C)	Reference
Calcium alginate	entrapment	4.2[b]	5.0	50–80	[39]
Alginate gel	entrapment	113[b]	nd[c]	nd[c]	[40]
Glutaraldehyde-Calcium alginate	entrapment	0.91[b]	4.0–5.5	55–70	[41]
Carrageenan gel	entrapment	40[b]	4.5–5.5	55	[42]
Gelatin hydrogel	entrapment	0.12[b]	–	60	[43]
PEO-co-PPy	entrapment	1389[b]	7.0	50	[24]
CP-co-PPy	entrapment	701[b]	6.0	50	
Sodium alginate	entrapment	106.14[b]	5.5	45	[44]
Calcium alginate	entrapment	4.8[b]	4.0	50	[45]
Poly(GMA-MMA)-PEI	adsorption	97	5.5–6.0	35–40	[46]
Duolite A-568	adsorption	25	4.9	40	[3]
D-sorbitol cinnamic ester	adsorption	2.35[b]	5.0	40	[47]
PAN/PANI	adsorption	95	5.0–6.0	45–55	[48]
chitosan-γ-Fe_2O_3	adsorption	60.8[b]	5.0	60	[7]
MANAE-agarose	adsorption	145	nd[c]	55	[49]
MANAE-agarose + glutaraldehyde	adsorption + cross-linking	90	nd[c]	45–55	
agarose + glutaraldehyde	covalent	125	nd[c]	45–55	
montmorillonite K-10	adsorption	5.1[b]	6.0	60	[50]
montmorillonite K-10-APTES	covalent	6.6[b]	5.0	60	
GA-N-CSMG	covalent	340[b]	4.0	55	[26]
Crystalline cellulose (Avicel)	covalent	10.3[b]	5.5	45	[51]
Poly(MA-alt-H-1)	covalent	16.4[b]	8.0	55	[52]
PMTM–PTAA	covalent	133	4.5	55	[53]
Nylon-6	covalent	158.73[b]	5.5	25	[54]
Crystalline cellulose (Avicel)	covalent	20.6[b]	5.5	30	[55]
Nylon-6	covalent	456[b]	5.5	30	
PU	covalent	65	5.0	50	[25]
Ferromagnetic azide-Dacron	covalent	1053	4.5	50	
mDE-APTES	covalent	3358	4.5	45	This work

[a] One unit (U) is defined as 1 μmol of substrate per mL during 1 min per mg of protein.
[b] Value calculated from paper data.
[c] nd means not determined.

ity). It is worthwhile to mention that the analysis of the interaction factors of second order by the square plot of predicted means is in concordance with the above result. The statistical combination of the independent variables in coded values along with the experimental response was presented in Table 2. The obtained mathematical model is expressed by the following equation:\

$$y = 29.38 - 7.93X_2 + 4.93X_3 - 18.30X_4 + 5.72X_1X_2 + 5.76X_1X_4 - 2.15X_2X_3 + 5.17X_2X_4 - 2.79X_3X_4 + 3.14X_1X_2X_3 - 3.91X_1X_2X_4 + 0.97X_1X_3X_4 + 3.11X_2X_3X_4$$

where percentage specific activity (y) is related to pH (X_1), temperature (X_2), sucrose concentration (X_3) and invertase concentration (X_4). The statistical significance of this equation was controlled by analysis of variance (ANOVA). According to ANOVA analysis only X_2 (temperature), X_3 (sucrose concentration), X_4 (invertase concentration), X_1X_2, X_1X_4 and X_2X_4 were the most significant parameters. The coefficient of determination ($R^2 = 0.9798$) indicated that the accuracy of the model was adequate. The results also showed that there is not lack of fit ($p = 0.0792$) and this was an evidence to display the validity of the model. A high accordance among the predicted and experimental percentage specific activities is observed in Fig. 3. Moreover, the raw residuals *versus* observed values plot showed that residuals are randomly assigned. As result of this experimental design, the run 5 (pH 4.5; temperature 45 °C; sucrose concentration, 0.25 mol L^{-1} and invertase concentration, 0.05 mg mL^{-1}) presented the best operational conditions for sucrose hydrolysis process by mDE-APTES-invertase. Even as, the temperature, sucrose concentration and invertase concentration were the most important factors that influenced the response significantly, other factors such as pH might affect the sucrose hydrolysis by immobilized invertase. The support structure and/or biomolecule; immobilization method as well as conditions of reaction medium are some of the reasons that influence in the choice of factors affecting the response. Therefore, Table 3 provides a comparison of the sucrose hydrolysis under different conditions by immobilized invertase on several matrices present in the literature. In the present study, the mDE-APTES-invertase presented the highest specific activity (3358 U mg^{-1} protein) in comparison to the values of the other studies. The works that reached the highest specific activities found in the literature used as matrix for invertase immobilization the poly(ethyleneoxide)/polypyrrole (PEO-co-PPy) with a specific activity equal to 1389 U mg^{-1} protein and the Ferromagnetic azide-Dacron with 1053 U mg^{-1} protein [24,25]. The other derivatives presented in Table 3 yielded specific activities in the range from 0.12 to 701 U mg^{-1} protein. The higher performance of mDE-APTES nanoparticles may be due to the high specific surface and porosity providing a larger area for the attachment of the enzyme. The covalent immobilization also provided a tight binding with resistance to the reaction environment.

Table 3 shows the optimal pH and temperature in the range of 4.0–8.0 and 25–80 °C, respectively. In this work, the results for pH and temperature obtained were similar to those reported by David et al. [26], however, the mDE-APTES-invertase showed almost 10-fold increase for specific activity. The authors found an optimum acid pH for immobilized invertase due to the basic nature of amino functionalized porous silica matrix. The matrix employed (magnetic diatomaceous earth) in this work presents also a basic nature due to treatment with APTES. Marquez et al. [3] reported a maximum response (enzymatic activity) at 40 °C and pH 4.9 for immobilized invertase on the ion exchanging resin Duoltite A-568 through of a central composite design that are close to those found in this work.

3.3. Thermal stability

Many studies about immobilized enzymes have shown that its

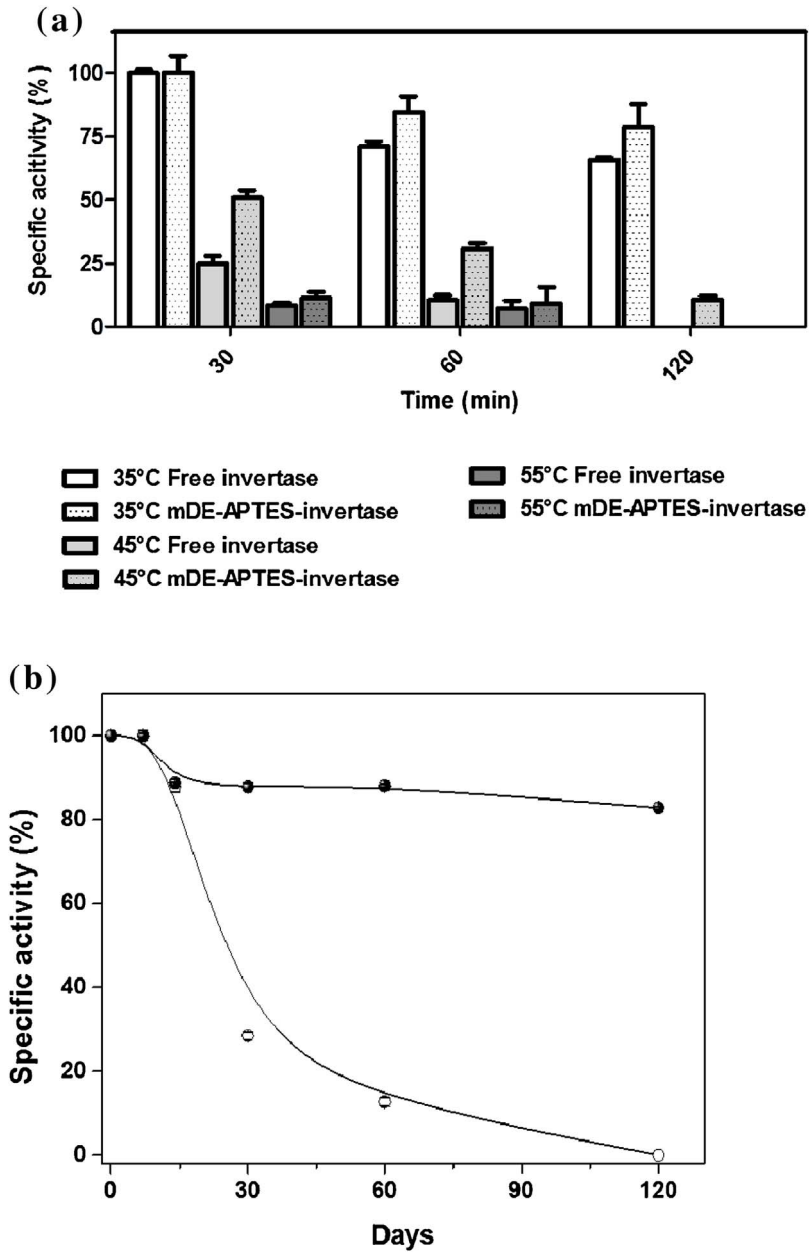

Fig. 4. (a) Thermal stability of free (clear bar) and immobilized (dot-filled bar) invertase at different temperatures and times. (b) Effect of storage stability on the activity of free (○) and immobilized (●) invertase on mDE nanoparticles.

activity and stability can differ from those of free enzyme [27]. Therefore, the thermal stability of mDE-APTES-invertase was compared with that of free enzyme (Fig. 4a). The best performance was observed at 45 °C for 30 min where the immobilized derivative showed 2.0-fold more resistance than the free enzyme. In addition, a good performance was displayed at 35 °C and 45 °C for 60 min for the immobilized derivative (85% and 31%, respectively) in comparison to the free enzyme (71% and 11%, respectively). At 45 °C the free form was inactivated at a much faster rate than the immobilized form but both enzymatic preparations at 55 °C lost their initial activity after 120 min treatments. We conclude that thermal stability of the mDE-APTES-invertase was better than the free invertase probably due to the covalent bond formation that might reduce the conformational flexibility of the enzyme and make it more stable against temperature changes [28]. Other authors also observed that after immobilization there was an improvement in thermal stability of enzyme [29–31].

3.4. Storage stability

In fact, immobilization ties the enzyme into a more stable position in comparison to the free enzyme as showed in Fig. 4b**.** After storage at 4 °C for 30 days, the specific activities were found to be 28 and 88% of the initial activity values for free and immobilized enzyme, respectively. The mDE-APTES-invertase presented a retained activity around 83% for 120 days storage period whereas the free enzyme lost all of its activity in the same period. The results showed a good storage stability of the immobilized derivative, and this can be attributed to the stability of the enzyme being enhanced by reducing its denaturation rate after immobilization [28]. Akgöl et al. [32] also observed an increase of storage stability of the immobilized invertase onto magnetic polyvinylalcohol microspheres. Authors reported that the immobilized derivative retained 62% of its initial activity after 28 days. Danisman et al. [33] after immobilizing invertase on microporous pHEMA-GMA membrane observed 78% of activity retention at the 35th day of storage. Here, mDE-APTES-invertase retained above 80% at the 120th day of

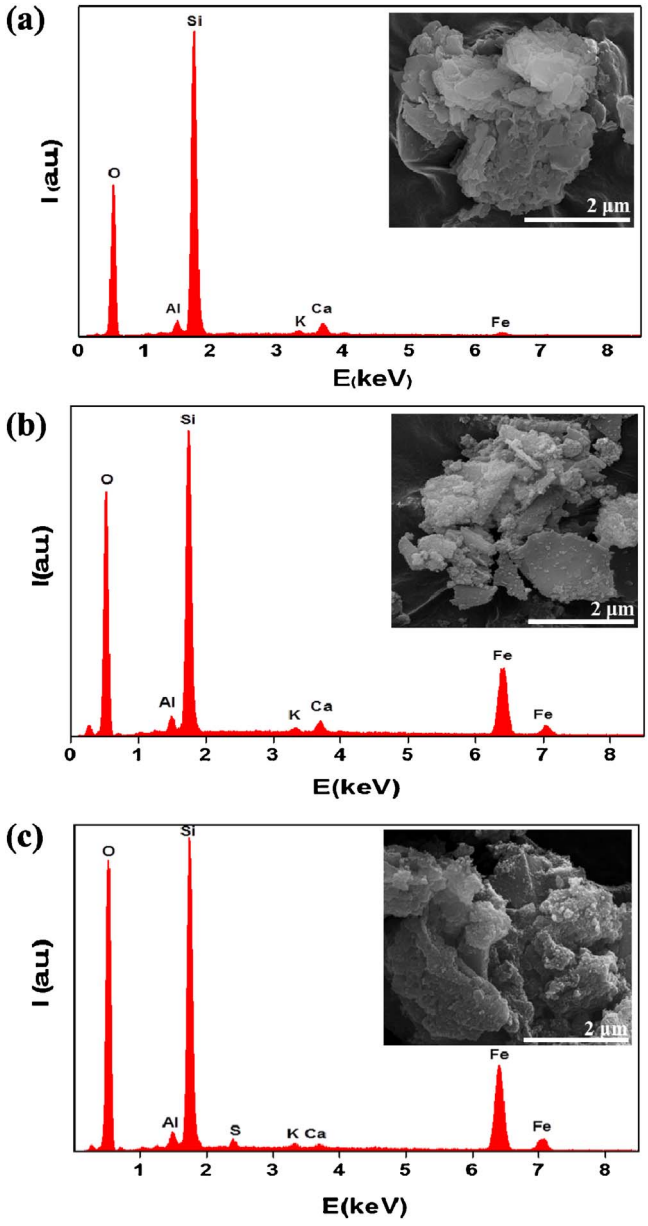

Fig. 5. EDS analysis of (a) raw DE, (b) mDE composite and (c) mDE-APTES-invertase. The inset shows the SEM photomicrographs for each sample (scale bar = 2 µm).

storage, which makes the mDE nanoparticles an attractive matrix for invertase immobilization as well as other enzymes.

3.5. Reusability of mDE-APTES-invertase

The reusability of the mDE-APTES-invertase in short and long term is shown in Fig. S2 (See Supplementary material). After ten cycles the immobilized derivative retained more than 60% of residual activity (Fig. S2a). The decrease of the activity by the mDE-APTES-invertase may be attributed to loss of magnetic nanoparticles during the washing process between each cycle. Raj et al. [31] reported the appreciable reusability of the immobilized invertase on nanogel-matrix up to eight cycles, but the relative activity decreased to 11.03% after the 9th cycle. The reuse in long term for the mDE-APTES-invertase was assessed up to 120 days. The results showed that immobilized derivative maintained 64% and 50% of residual activity after 30 and 120 days at 4 °C, respectively (Fig. S2b). Tuncagil et al. [34] exhibited a retain activity of 30 and 40% in the first 10 days for the immobilized invertase onto random and block copolymers, respectively, with loss of its activities at

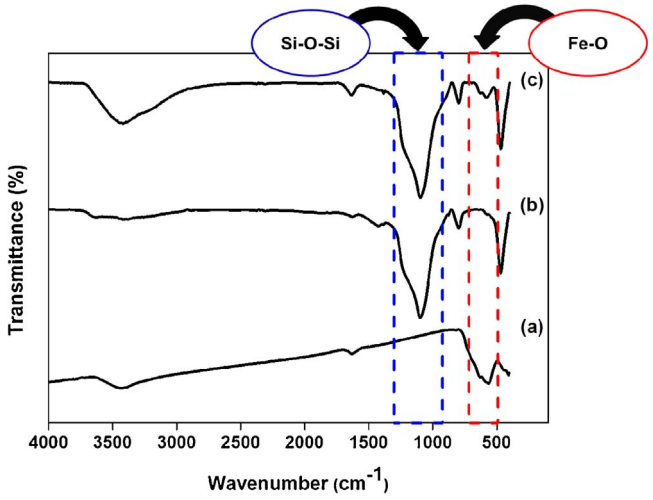

Fig. 6. FTIR spectra of (a) magnetite, (b) raw DE and (c) mDE composite. Dash lines highlight the presence of main functional group for magnetite and mDE (red; Fe-O bond), and DE and mDE (blue; Si—O—Si bond).

Table 4
Specific surface area, pore volume and mean pore size of the samples.

Sample	S_{BET} ($m^2\ g^{-1}$)	Pore Volume ($cm^3\ g^{-1}$)	Pore Size (nm)
DE	32.9	0.08	11.8
mDE	56.6	0.16	12.7
mDE-APTES-invertase	41.2	0.12	11.9

the end of 25 days. The results obtained in this work showed that the support and immobilization protocol are efficient for enzyme stability.

3.6. Characterization

In this work, mDE nanoparticles (12 nm) were synthesized by co-precipitation method as proposed by Cabrera et al. [18]. The XRD analysis and Mössbauer spectroscopy supported the presence of only magnetite, as iron phase, and DE in the magnetic composite. A good magnetic response and superparamagnetic behavior were also observed for the mDE composite [18]. These features are very important for the magnetic bio-separation technology because the magnetite has a better response against an external magnetic field applied when compared with others iron oxides (maghemite – γ-Fe_2O_3, and hematite – α-Fe_2O_3).

Fig. 5 shows EDS analysis and SEM photomicrographs (inset) of the samples. The morphology of the DE particles was irregular, and showed a typical sheet-like structure. The EDS spectrum for the DE (Fig. 5a) showed the expected peaks of Si and O, and other elements (Al, K, Ca, Fe). The magnetic composite (mDE) displayed a different texture in which the layers seemed more irregular and a high surface roughness (Fig. 5b). This roughness can be attributed to aggregates of magnetite on DE surface. Its EDS spectrum exhibited an increase in the signal corresponding to Fe, supporting the presence of magnetite on the mDE. The addition of invertase on mDE further changed the morphology of the material (Fig. 5c). The layer formation and agglomeration that occurred between magnetic particles and enzyme were observed. Probably, this surface alteration is due to the highly polymeric material of the enzyme covering the magnetic particles. This finding has been reported by Gopinath and Sugunan [35] working with immobilized enzymes including invertase. It is worthwhile to register the presence of S in the EDS of mDE-APTES-invertase which is an evidence of the presence of enzymes due to disulfide bonds and amino acid residues containing sulfur in its structure (Fig. 5c).

The FTIR spectra of magnetite, DE and mDE are shown in Fig. 6. The magnetite spectrum exhibited absorption bands at around 630 and

583 cm^{-1}, characteristic of the Fe-O bond [36]. The bands near to 3421 and 1638 cm^{-1} are ascribed to the hydroxyl, characteristic peaks of water adsorbed on the surface or the OH-stretching bands and its bending vibration peak [37]. The spectral band intensities of DE were at 3648, 1630, 1200, 1097, 800 and 470 cm^{-1}. The band at 3648 cm^{-1} (weak) is due to free surface silanol group (Si—OH); the bands at 1200 and 1097 cm^{-1} (strong and broad) are mainly due to the siloxane (Si—O—Si) stretching, while the bands at 800 and 470 cm^{-1} (strong and narrow) occur due to (Si—O) stretching of silanol group and (Si—O—Si) bending vibration, respectively [12,38]. After magnetization process, the mDE spectrum showed the same absorption bands of Fe—O bond around 633 and 583 cm^{-1}, which supported the presence of magnetite particles.

The BET test was conducted to determine textural parameters, such as BET surface area, pore volume and mean pore size of samples. Table 4 displays the textural parameters for all samples. As result of the magnetization process the mDE presented a higher surface area and pore volume compared to DE. This increase can be indicative of the creation of open pores on the diatomite backbone surface, as a consequence of magnetite deposits on the surface of DE particles. Furthermore, the immobilization process can be improved because the enzymes will have more chemical sites (-NH_2; amino group from APTES functionalization) available on mDE surface for covalent binding. Al-Degs et al. [38] reported that the surface area of diatomite depends mainly on the hydroxyl groups (—OH) present on the surface of this material. The authors showed values of 33 and 80 $m^2\,g^{-1}$ of surface area for the diatomite and manganese-diatomite, respectively. After immobilization process, a decrease in the specific surface area was observed. Probably because the material pores were partially covered during the immobilization of enzymes on the mDE. The values of pore size for the samples are in the range of mesoporous solid (between 2 and 50 nm) according to IUPAC. The mDE composite displayed pores with slit-shaped openings as depicted by the type II of the adsorption-desorption isotherms and the H3 hysteresis loops (data not shown).

The physicochemical characterization allowed to state that the mDE composite was synthesized with success and this affirmation was supported by the SEM-EDS and FTIR techniques. Moreover, BET test suggested that mDE composite presented characteristics of a mesoporous solid.

4. Conclusion

This work proposes magnetic diatomaceous earth nanoparticles as a matrix for invertase immobilization. Experimental designs allowed establishing the best operational conditions for invertase immobilization process. The immobilized derivative presented a residual specific activity of 92.5% compared to the free enzyme. Sucrose hydrolysis rate by this derivate was 2.42-fold higher than those reported in the literature. Thermal and storage stability were found to be respectively, 35 °C for 60 min (85% retained activity) and at 120th storage day (80% retained activity). Residual activity higher than 60% and 50% were observed for the enzymatic derivative after reuse in short and long term, respectively. Physicochemical characterization by SEM-EDS, FTIR and BET test corroborated the magnetic enzymatic composite synthesis.

Acknowledgments

This work was financially supported by the Brazilian Agencies:CAPES (Coordenação de Aperfeiçoamento de Pessoal de Nível Superior) and CNPq (Conselho Nacional de Desenvolvimento Científico e Tecnológico). The physicochemical characterizations were carried out at CETENE (Centro de Tecnologias Estratégicas do Nordeste). Authors are also thankful to Professor Benício de Barros Neto (*in memoriam*) for this invaluable collaboration and knowledge transmitted in the statistical area.

Appendix A. Supplementary data

Supplementary data associated with this article can be found, in the online version, at http://dx.doi.org/10.1016/j.btre.2017.03.001.

References

[1] J. Bryjak, J. Liesiene, V. Štefuca, Man-tailored cellulose-based carriers for invertase immobilization, Cellulose 15 (4) (2008) 631–640.
[2] M.M.M. Elnashar, Immobilized molecules using biomaterials and nanobiotechnology, J. Biomater. Nanobiotechnol. 1 (1) (2010) 61–77.
[3] L.D.S. Marquez, B.V. Cabral, F.F. Freitas, V.L. Cardoso, E.J. Ribeiro, Optimization of invertase immobilization by adsorption in ionic exchange resin for sucrose hydrolysis, J. Mol. Catal. B: Enzym. 51 (3–4) (2008) 86–92.
[4] L. Cao, Immobilised enzymes: science or art? Curr. Opin. Chem. Biol. 9 (2) (2005) 217–226.
[5] S.M. Kotwal, V. Shankar, Immobilized invertase, Biotechnol. Adv. 27 (4) (2009) 311–322.
[6] A. Margetić, Z. Vujčić, Comparative study of stability of soluble and cell wall invertase from Saccharomyces cerevisiae, Prep. Biochem. Biotechnol. 47 (3) (2017) 305–311.
[7] P.P. Waifalkar, S.B. Parit, A.D. Chougale, S.C. Sahoo, P.S. Patil, P.B. Patil, Immobilization of invertase on chitosan coated γ-Fe2O3 magnetic nanoparticles to facilitate magnetic separation, J. Colloid Interface Sci. 482 (2016) 159–164.
[8] U. Andjelković, A. Milutinović-Nikolić, N. Jović-Jovičić, P. Banković, T. Bajt, Z. Mojović, Z. Vujčić, D. Jovanović, Efficient stabilization of Saccharomyces cerevisiae external invertase by immobilisation on modified beidellite nanoclays, Food Chem. 168 (2015) 262–269.
[9] S. Kaufhold, R. Dohrmann, C. Ulrichs, Shelf life stability of diatomites, Appl. Clay Sci. 41 (3–4) (2008) 158–164.
[10] W.-T. Tsai, C.-W. Lai, K.-J. Hsien, Characterization and adsorption properties of diatomaceous earth modified by hydrofluoric acid etching, J. Colloid Interface Sci. 297 (2) (2006) 749–754.
[11] C. Nattrass, C.J. Horwell, D.E. Damby, A. Kermanizadeh, D.M. Brown, V. Stone, The global variability of diatomaceous earth toxicity: a physicochemical and in vitro investigation, J. Occup. Med. Toxicol. (London, England) 10 (2015) 1–16.
[12] H. Maeda, E.H. Ishida, Hydrothermal preparation of diatomaceous earth combined with calcium silicate hydrate gels, J. Hazard. Mater. 185 (2–3) (2011) 858–861.
[13] D. Losic, Y. Yu, M.S. Aw, S. Simovic, B. Thierry, J. Addai-Mensah, Surface functionalisation of diatoms with dopamine modified iron-oxide nanoparticles: toward magnetically guided drug microcarriers with biologically derived morphologies, Chem. Commun. 46 (34) (2010) 6323–6325.
[14] H. Alijani, M.H. Beyki, Z. Shariatinia, M. Bayat, F. Shemirani, A new approach for one step synthesis of magnetic carbon nanotubes/diatomite earth composite by chemical vapor deposition method: application for removal of lead ions, Chem. Eng. J. 253 (2014) 456–463.
[15] Y. He, W. Zhang, P. Rao, P. Jin, Performance of diatomite/iron oxide modified nonwoven membrane used in membrane bioreactor process for wastewater reclamation, Water Sci. Technol. 70 (3) (2014) 533–539.
[16] W. Xiong, J. Peng, Development and characterization of ferrihydrite-modified diatomite as a phosphorus adsorbent, Water Res. 42 (19) (2008) 4869–4877.
[17] P. Yuan, D. Liu, M. Fan, D. Yang, R. Zhu, F. Ge, J. Zhu, H. He, Removal of hexavalent chromium [Cr(VI)] from aqueous solutions by the diatomite-supported/unsupported magnetite nanoparticles, J. Hazard. Mater. 173 (1–3) (2010) 614–621.
[18] M. Cabrera, J.C. Maciel, J. Quispe-Marcatoma, B. Pandey, D.F.M. Neri, F. Soria, E. Baggio-Saitovitch, L.B. Carvalho Jr., Magnetic composites from minerals: study of the iron phases in clay and diatomite using Mössbauer spectroscopy, magnetic measurements and XRD, Hyperfine Interact. 224 (1–3) (2014) 197–204.
[19] M. Khayet, C. Cojocaru, G. Zakrzewska-Trznadel, Response surface modelling and optimization in pervaporation, J. Membr. Sci. 321 (2) (2008) 272–283.
[20] O.H. Lowry, N.J. Rosebrough, A.L. Farr, R.J. Randall, Protein measurement with the folin phenol reagent, J. Biol. Chem. 193 (1) (1951) 265–275.
[21] R. Bergamasco, F.J. Bassetti, F.F.d Moraes, G.M. Zanin, Characterization of free and immobilized invertase regarding activity and energy of activation, Braz. J. Chem. Eng. 17 (2000) 873–880.
[22] G. Sanjay, S. Sugunan, Invertase immobilised on montmorillonite: reusability enhancement and reduction in leaching, Catal. Commun. 6 (1) (2005) 81–86.
[23] D. Brand, A. Pandey, J.A. Rodriguez-Leon, S. Roussos, I. Brand, C.R. Soccol, Packed bed column fermenter and kinetic modeling for upgrading the nutritional quality of coffee husk in solid-state fermentation, Biotechnol. Prog. 17 (6) (2001) 1065–1070.
[24] H.B. Yildiz, M. Kamaci, H. Azak, O. Secgin, O. Suer, A comparative study: immobilization of yeast cells and invertase in poly(ethyleneoxide) electrodes, J. Mol. Catal. B: Enzym. 91 (2013) 52–58.
[25] P.G. Cadena, R.A.S. Jeronimo, J.M. Melo, R.A. Silva, J.L. Lima Filho, M.C.B. Pimentel, Covalent immobilization of invertase on polyurethane, plast-film and ferromagnetic Dacron, Bioresour. Technol. 101 (6) (2010) 1595–1602.
[26] A.E. David, N.S. Wang, V.C. Yang, A.J. Yang, Chemically surface modified gel (CSMG): an excellent enzyme-immobilization matrix for industrial processes, J. Biotechnol. 125 (3) (2006) 395–407.
[27] C. Mateo, V. Grazu, B.C. Pessela, T. Montes, J.M. Palomo, R. Torres, F. Lopez-Gallego, R. Fernandez-Lafuente, J.M. Guisan, Advances in the design of new epoxy supports for enzyme immobilization-stabilization, Biochem. Soc. Trans. 35 (Pt 6) (2007) 1593–1601.
[28] H. Altinok, S. Aksoy, H. Tümtürk, N. Hasirci, Covalent immobilization of invertase

on chemically activated poly(styrene-2-hydroxyethyl methacrylate) microbeads, J. Food Biochem. 32 (3) (2008) 299–315.
[29] L. Amaya-Delgado, M.E. Hidalgo-Lara, M.C. Montes-Horcasitas, Hydrolysis of sucrose by invertase immobilized on nylon-6 microbeads, Food Chem. 99 (2) (2006) 299–304.
[30] G. Bayramoğlu, M. Karakışla, B. Altıntaş, A.U. Metin, M. Saçak, M.Y. Arıca, Polyaniline grafted polyacylonitrile conductive composite fibers for reversible immobilization of enzymes: stability and catalytic properties of invertase, Process Biochem. 44 (8) (2009) 880–885.
[31] L. Raj, G.S. Chauhan, W. Azmi, J.H. Ahn, J. Manuel, Kinetics study of invertase covalently linked to a new functional nanogel, Bioresour. Technol. 102 (3) (2011) 2177–2184.
[32] S. Akgöl, Y. Kaçar, A. Denizli, M.Y. Arıca, Hydrolysis of sucrose by invertase immobilized onto novel magnetic polyvinylalcohol microspheres, Food Chem. 74 (3) (2001) 281–288.
[33] T. Danisman, S. Tan, Y. Kacar, A. Ergene, Covalent immobilization of invertase on microporous pHEMA–GMA membrane, Food Chem. 85 (3) (2004) 461–466.
[34] S. Tuncagil, S. Kıralp, S. Varıs, L. Toppare, Immobilization of invertase on a conducting polymer of 1-(4-nitrophenyl)-2 5-di(2-thienyl)-1H-pyrrole, React. Funct. Polym. 68 (3) (2008) 710–717.
[35] S. Gopinath, S. Sugunan, Enzymes immobilized on montmorillonite K 10: effect of adsorption and grafting on the surface properties and the enzyme activity, Appl. Clay Sci. 35 (1–2) (2007) 67–75.
[36] B. Feng, R.Y. Hong, L.S. Wang, L. Guo, H.Z. Li, J. Ding, Y. Zheng, D.G. Wei, Synthesis of Fe3O4/APTES/PEG diacid functionalized magnetic nanoparticles for MR imaging, Coll. Surf. A 328 (1–3) (2008) 52–59.
[37] V.S. Zaitsev, D.S. Filimonov, I.A. Presnyakov, R.J. Gambino, B. Chu, Physical and chemical properties of magnetite and magnetite-polymer nanoparticles and their colloidal dispersions, J. Colloid Interface Sci. 212 (1) (1999) 49–57.
[38] Y. Al-Degs, M.A.M. Khraisheh, M.F. Tutunji, Sorption of lead ions on diatomite and manganese oxides modified diatomite, Water Res. 35 (15) (2001) 3724–3728.
[39] A. Milovanović, N. Božić, Z. Vujčić, Cell wall invertase immobilization within calcium alginate beads, Food Chem. 104 (2007).
[40] T.K.H. Vu, V.V.M. Le, Biochemical studies on the immobilization of the enzyme invertase (EC.3.2.1.26) in alginate gel and its kinetics, ASEAN Food J. 15 (2008) 73–78.
[41] Z. Vujčić, A. Milovanović, N. Božić, B. Dojnov, M. Vujčić, U. Andjelković, N. Lončar, Immobilization of cell wall invertase modified with glutaraldehyde for continuous production of invert sugar, J. Agric. Food Chem. 58 (22) (2010) 11896–11900.
[42] W.A. Mahmood, Hydrolysis of sucrose by immobilized Saccharomyces cerevisiae Invertase, Mesop. J. Agric. 38 (2010) 1–10.
[43] Z. Vujčić, Z. Miloradović, A. Milovanović, N. Božić, Cell wall invertase immobilisation within gelatin gel, Food Chem. 126 (2011).
[44] R. Mouelhi, F. Abidi, S. Galai, M.N. Marzouki, Immobilized Sclerotinia sclerotiorum invertase to produce invert sugar syrup from industrial beet molasses by product, World J. Microbiol. Biotechnol. 30 (3) (2014) 1063–1073.
[45] J.A. Solís-Fuentes, E. Raga-Carbajal, M.C. Durán-de-Bazúa, Direct sucrose hydrolysis in sugarcane juice with immobilized invertase: multi-response optimization using desirability function on conversion and reactor volumetric productivity, Sugar Tech. 17 (3) (2015) 266–275.
[46] M.Y. Arıca, G. Bayramoğlu, Invertase reversibly immobilized onto polyethylenimine-grafted poly(GMA–MMA) beads for sucrose hydrolysis, J. Mol. Catal. B: Enzym. 38 (3–6) (2006) 131–138.
[47] V. Vallejo-Becerra, M.E. Marín-Zamora, J.M. Vásquez-Bahena, F. Rojas-Melgarejo, M.E. Hidalgo-Lara, P.A. García-Ruiz, Immobilization of recombinant invertase (re-INVB) from zymomonas mobilis on d-Sorbitol cinnamic ester for production of invert sugar, J. Agric. Food Chem. 56 (4) (2008) 1392–1397.
[48] G. Bayramoglu, M. Karakisla, B. Altintas, A.U. Metin, M. Sacak, M.Y. Arica, Polyaniline grafted polyacylonitrile conductive composite fibers for reversible immobilization of enzymes: stability and catalytic properties of invertase, Process Biochem. 44 (2009).
[49] A.J. Goulart, A.F. dos Santos, O.L. Tavano, J.C. Vinueza, J. Contiero, R. Monti, Glucose and fructose production by saccharomyces cerevisiae invertase immobilized on MANAE-agarose support, J. Basic Appl. Pharm. Sci. 34 (2013) 169–175.
[50] G. Sanjay, S. Sugunan, Enhanced pH and thermal stabilities of invertase immobilized on montmorillonite K–10, Food Chem. 94 (2006).
[51] J.A. Santiago-Hernández, J.M. Vásquez-Bahena, M.A. Calixto-Romo, G.B. Xoconostle-Cázares, J. Ortega-López, R. Ruíz-Medrano, M.C. Montes-Horcasitas, M.E. Hidalgo-Lara, Direct immobilization of a recombinant invertase to Avicel by E. coli overexpression of a fusion protein containing the extracellular invertase from Zymomonas mobilis and the carbohydrate-binding domain CBDCex from Cellulomonas fimi, Enzyme Microb. Technol. 40 (1) (2006) 172–176.
[52] H. Mazi, E. Emregul, Z.M.O. Rzaev, G. Kibarer, Preparation and properties of invertase immobilized on a poly(maleic anhydride-hexen-1) membrane, Journal of Biomaterials Science, Polym. Ed. 17 (7) (2006) 821–835.
[53] N. Dizge, O. Gunaydin, F. Yilmaz, A. Tanriseven, Immobilization of invertase onto poly(3-methylthienyl methacrylate)/poly(3-thiopheneacetic acid) matrix, Biochem. Eng. J. 40 (1) (2008) 64–71.
[54] V. Vallejo-Becerra, J.M. Vásquez-Bahena, J.A. Santiago-Hernández, M.E. Hidalgo-Lara, Immobilization of the recombinant invertase INVB from Zymomonas mobilis on Nylon-6, J. Ind. Microbiol. Biotechnol. 35 (2008).
[55] M. de los Ángeles Calixto-Romo, J.A. Santiago-Hernández, V. Vallejo-Becerra, L. Amaya-Delgado, M. del Carmen Montes-Horcasitas, M.E. Hidalgo-Lara, Expression, purification and immobilization of the intracellular invertase INVA, from Zymomonas mobilis on crystalline cellulose and Nylon-6, J. Ind. Microbiol. Biotechnol. 35 (11) (2008) 1455.